

A Study of Some New Features for the Palmprint Based Authentication

Madasu Hanmandlu, Ritu Vijay, Neha Mittal

Abstract—This paper presents an authentication system based on palmprint. The Region of interest (ROI) is extracted from the palmprint image. A tangent is drawn by finding the curves between fingers. The perpendicular bisector of this tangent divides the rectangular area enclosing the palmprint into two equal parts. For the purpose of feature extraction, ROI is divided into a suitable number of non-overlapping windows of different sizes and three types of features, viz. Sigmoid, Energy and Entropy features are extracted. These three sets of features are used for the authentication of users using Euclidean Distance and Support Vector Machine (SVM) as the classifiers.

Index Terms— Sigmoid, Energy and Entropy feature, Support Vector Machine, palmprint, authentication

I. INTRODUCTION

The palmprint as a biometric modality is gaining acceptance in the field of biometrics. As compared to other biometric modalities, it is bestowed with enormous information serving as its discriminating power. We will discuss a few important contributions made on this modality.

Matching of palmprints in [5] deals with the feasibility of identifying a person based on a set of features extracted along the prominent palm lines (and the associated line orientation) from a palmprint. Next a decision is made whether two palmprints belong to the same hand by computing a matching score between the corresponding sets of features of the reference and test palmprints. These two sets of features/orientations are matched using point matching technique which takes into account the nonlinear deformations as well as the outliers present in the two sets.

An important indexing algorithm is proposed in [10] based on the palmprint classification. This algorithm uses a novel representation involving a two-stage classifier that provides the even-distributed categories. The representation scheme is directly derived from the principal line structures. This scheme does not use wrinkles and singular points and is capable of tolerating poor image quality.

In this paper, we will explore features such as Sigmoid, Energy and Entropy extracted from a palmprint. An effort is

made to bank upon on two counts: An efficient extraction of Region of Interest (ROI) and an effective feature selection.

The organization of the paper is as follows: Section 2 presents the extraction of ROI. The extraction of sigmoid, energy and entropy features is described in Section 3. Matching and results of implementation are described in Sections 4 and 5 respectively. Finally conclusions are given in Section 6.

II. ROI EXTRACTION

2.1 The Preprocessing for ROI extraction

The following steps outline the ROI extraction from a palmprint:

1. Take the original image (See Fig. 1) and convert it from RGB to gray scale.
2. Crop a fixed section of the image not touching the glass (See Fig. 2).
3. Rotate this section based on the type of hand— left or right so that the image is in the specified direction.
4. Find the histogram of the image.
5. Compute the moving average of the histogram, and find the minimum of this average. The point of minimum provides us with the threshold for binarizing the image. The binary conversion [2] is such that it inverts the image, i.e. all dark regions including the cavities between fingers get bright whereas the hand region becomes black
6. Application of the morphological operators removes very small connected regions including any holes in the white connected regions as shown in Fig.2.
7. Search for the cavities on the left side of the binary image. Rotating the hand the two cavities— one between the little finger and the ring finger, and another between the middle finger and the index finger are detected.
8. The Laplacian edge detector is applied on the fingers to get the contours of the cavities.
9. A tangent is drawn between the two contours of the cavities in Fig. 4 such that all the points of both the contours lie on one side of the tangent.
10. The perpendicular bisector of this tangent is taken as the x-axis and the tangent is taken as the y-axis to form a coordinate system that facilitates earmarking the ROI.
11. The ROI is rotated and resized to save as a file.

Manuscript received March 01, 2011; revised April 05, 2011.

Prof. Madasu Hanmandlu is with EE Department, I.I.T. Delhi, New Delhi-110016, INDIA (e-mail: mhmandlu@ee.iitd.ernet.in).

Dr. Ritu Vijay is with Banasthali University, Banasthali, Rajasthan, INDIA. (e-mail: rituvijay1975@yahoo.co.in).

Neha Mittal is with the Electronics and Communication Engineering Department, J.P. Institute of Engineering & Technology, Meerut, UP, INDIA, (e-mail: nehamittal2008@gmail.com).



Fig. 1: A typical Palmprint



Fig. 2: Cropped section of image in Fig.1



Fig. 3: Binarized Image

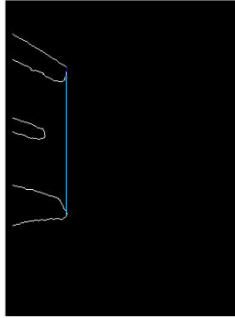


Fig. 4: A common tangent between two curves

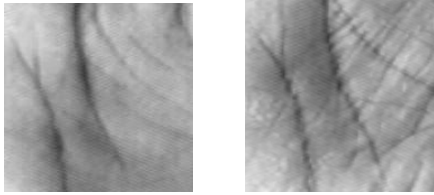


Fig. 5: The extracted ROI of palmprint

III. FEATURE EXTRACTION

The ROI is partitioned into a fixed number of non overlapping windows. From each of these windows features are extracted. We have made a choice of sigmoid, energy and entropy as our three feature types for trail on the palmprints. While deriving the three types of features, the average intensity and maximum intensity of sub image are required. We will now elaborate on each feature type.

3.1 Sigmoid Features

Here the sigmoid function is used to generate features.

1. The average intensity I_{avg} is calculated from

$$I_{avg} = \frac{\sum_{i=1}^m \sum_{j=1}^n I(i, j)}{m \times n} \quad (1)$$

2. The maximum intensity, I_{max} is found.
3. The sigmoid feature indicated by sig is obtained as

$$Sig = \frac{I_{avg}}{1 + \exp\left(-\frac{I_{avg}}{I_{max}}\right)} \quad (2)$$

3.2 Energy Features

This feature gives the distribution of energy in the sub windows of ROI. Energy features are derived as follows:

1. The average intensity I_{avg} is now modified to remove the center pixel intensity:

$$I_{avg} = \frac{\left(\sum_{i=1}^m \sum_{j=1}^n I(i, j)\right) - C}{(m \times n) - 1} \quad (3)$$

C is the gray level intensity of center pixel.

2. The maximum intensity, $I_{max}(i, j)$ is found .
3. The fuzzy membership function μ is taken as

$$\mu_{ij} = 1 - \frac{|I(i, j) - I_{avg}|}{I_{max}} \quad (4)$$

4. The Energy is computed from

$$E_g = \frac{\sum_{i=1}^m \sum_{j=1}^n \mu_{ij}^2}{m \times n} \quad (5)$$

3.3 Entropy Features

Entropy is a measure of information of source symbols which in the case of palmprints turn out to be the gray levels.

1. The maximum intensity, $I_{avg}(i, j)$ is in equation(3).
2. The membership function μ is as in equation (4).
3. The Entropy function is as follows:

$$E_n = -\frac{1}{(m \times n) \log 2} \sum_{i=1}^m \sum_{j=1}^n (\mu_{ij} \log \mu_{ij} + |1 - \mu_{ij}| \log |1 - \mu_{ij}|) \quad (6)$$

where $(m \times n)$ are the total number of pixels in a window.

IV. MATCHING

4.1. Euclidean Distance Measure

Given two data sets of features corresponding to the training and testing samples, a matching algorithm ascertains the degree of similarity between them. The Euclidean distance is adopted as a measure of dissimilarity for matching the palmprints. Genuine scores are derived from the matching distances (Euclidean distance) between the same user and the imposter scores are calculated from the matching distances between two different users. The graph of receiver operating characteristic (ROC) is a plotted as GAR(Genuine Acceptance Rate) Vs. FAR(False Acceptance Rate).

4.2. Support Vector Machines

SVM operates on the principle of Structural Risk Minimization (SRM) [14, 15]. It constructs a hyper-plane or a set of hyper-planes on a high dimensional space for the classification of input features. Considering a two-class

problem to be solved by a SVM , we start with a training sample described by a set of features $x_i \in R^n$; n being the number of features belonging to one of the two classes designated by the label $y_i \in \{+1,-1\}$. The data to be classified by the SVM may not be linearly separable in the original feature space. In the linearly non-separable case the data is projected onto a higher dimensional feature space using Kernel function [8]

$$K(x_i, x_j) = \phi(x_i)^T \cdot \phi(x_j) \quad i, j = 1, 2, 3, \dots, N \quad (7)$$

where ϕ is the function that maps the data onto the higher dimensional space H . Next, SVM generates a hyper-plane in H with the decision boundary given by

$$f(x) = \sum_{i=1}^N y_i \alpha_i K(x, x_i) + b \quad (8)$$

where α_i is the non-negative Lagrange multiplier. A quadratic optimization problem is set up to solve for the unknown parameters. It is defined as:

Minimize:

$$L(w, b, \alpha) = \sum_{i=1}^n \alpha_i - \frac{1}{2} \sum_{i=1}^N \sum_{j=1}^N y_i y_j \alpha_i \alpha_j K(x_i, x_j)$$

$$\text{Subject to: } 0 \leq \alpha_i \leq C, i = 1, 2, 3, \dots, N \quad (9)$$

where the cost parameter, C controls the trade-off between the training errors and the rigid margins. A few kernel functions used in this study are:

Linear kernel:

$$K(x_i, x_j) = a \cdot x_i^T \cdot x_j + b \quad (10)$$

Radial basis function (RBF):

$$K(x_i, x_j) = \exp(-\gamma \|x_i - x_j\|^2) \quad (11)$$

Sigmoid kernel :

$$K(x_i, x_j) = \tanh(a \cdot x_i^T \cdot x_j + b) \quad (12)$$

Polynomial kernel function:

$$K(x_i, x_j) = (\alpha x_i^T x_j + c)^d \quad (13)$$

In the above the adjustable parameters are the slope (α), the constants a, b, c and the degree of polynomial d , which is varied in the polynomial kernel function. For the classification of the data LIBSVM [9] has been used. The values of the parameters are selected as $a=1, c=0, T=1$ and $d=1, 2$ and 3 .

V. RESULTS OF IMPLEMENTATION

We have used the IIT database containing 5 samples per user totaling $125 \times 5 = 625$ images and also the PolyU database containing 363 users with 6 samples for each user, totaling $363 \times 5 = 1815$ images. Several experiments are conducted by taking different combinations of training and testing samples. The size of window is also varied and the recognition rates corresponding to sigmoid, energy and entropy are obtained. The performance of sigmoid, energy and entropy features on three window sizes (5x5, 7x7, 9x9) using Euclidean classifiers and SVM classifiers is shown in Tables I-VI for both databases. Both sigmoid and entropy features have neck to neck competition. The energy features have slightly inferior performance. A comparison of the performance of the three feature types appears in the form of ROC plots in Figs. 11 and 12 corresponding to PolyU

and IITD databases respectively. These ROC's are made taking a window size of 9x9.

The entropy features yield GAR of 94.7% at FAR of 10^{-3} on PolyU database and GAR of 98.4% at FAR of 10^{-2} on IITD database for (4:1) at a window size of 9x9 with Euclidean classifier. The corresponding figures for (3:2) are GAR of 92.2% at FAR of 10^{-3} and GAR of 91.6% at a FAR of 10^{-2} on PolyU and IITD databases respectively on the same window size. The sigmoid features yield GAR of 97.8% at FAR of 10^{-3} on PolyU and GAR of 100% at FAR of 10^{-2} on IITD database for the window size of 9x9 at (4:1) and the corresponding figures at (3:2) are 94.3% GAR on PolyU and 92.2% GAR on IITD respectively at the same window size.

TABLE I
SIGMOID FEATURE ON IITD DATABASE

window size	ED % GAR at 10^{-2} FAR	SVM using different Polynomial Kernel functions		
		1 degree	2 degree	3 degree
(4:1)*				
5x5	100	100	100	100
7x7	100	100	100	100
9x9	100	100	96	96.8
(3:2)*				
5x5	92.5	100	99.6	99.2
7x7	93.2	100	96	100
9x9	92.2	92.8	92.8	91.6

TABLE II
SIGMOID FEATURE ON POLYU DATABASE

window size	ED % GAR at 10^{-3} FAR	SVM using different Polynomial Kernel functions		
		1 degree	2 degree	3 degree
(4:1)*				
5x5	96.7	99.72	100	100
7x7	97.5	99.72	99.72	100
9x9	97.8	99.72	97.52	98.89
(3:2)*				
5x5	94.5	99.31	99.03	99.03
7x7	94.2	99.17	99.03	99.03
9x9	94.3	99.17	97.24	97.24

The usefulness of the features can be judged from the comparative differences. For this purpose, we discuss the plots of Entropy features in Fig. 6 belonging to samples of two different users and in Fig. 7 those belonging to the same user to get an idea of how they differ. The differences between the features of two different users and the same users are depicted in Fig. 8. It can be clearly seen that the differences are prominent when the users are different as against the differences between the features of the same users.

TABLE IV
ENERGY FEATURE ON POLYU DATABASE

window size	ED	SVM using different Polynomial Kernel functions		
	% GAR at 10^{-3} FAR	1 degree	2 degree	3 degree
(4:1)*				
5x5	83.2	99.17	98.89	98.89
7x7	92	99.72	98.89	98.89
9x9	92.8	99.72	98.89	100
(3:2)*				
5x5	76.5	99.17	98.89	98.89
7x7	87.6	99.17	98.62	98.89
9x9	88.6	99.03	98.89	99.3

TABLE V
ENTROPY FEATURE ON IITD DATABASE

window size	ED	SVM using different Polynomial Kernel functions		
	% GAR at 10^{-2} FAR	1 degree	2 degree	3 degree
(4:1)*				
5x5	88	99.2	98.4	96.8
7x7	94.4	100	98.4	96.8
9x9	98.4	100	98.4	96
(3:2)*				
5x5	76.5	99.6	95.6	95.2
7x7	86.4	100	96.8	95.2
9x9	91.6	100	96.8	95.6

TABLE VI
ENTROPY FEATURE ON POLYU DATABASE

window size	ED	SVM using different Polynomial Kernel functions		
	% GAR at 10^{-3} FAR	1 degree	2 degree	3 degree
(4:1)*				
5x5	90.6	99.4	99.7	98.34
7x7	93.6	99.72	98.89	98.62
9x9	94.7	100	99.17	99.17
(3:2)*				
5x5	86.4	99.17	98.89	98.76
7x7	91.4	99.58	98.89	98.76
9x9	92.2	99.17	98.89	98.89

(train samples : test samples)

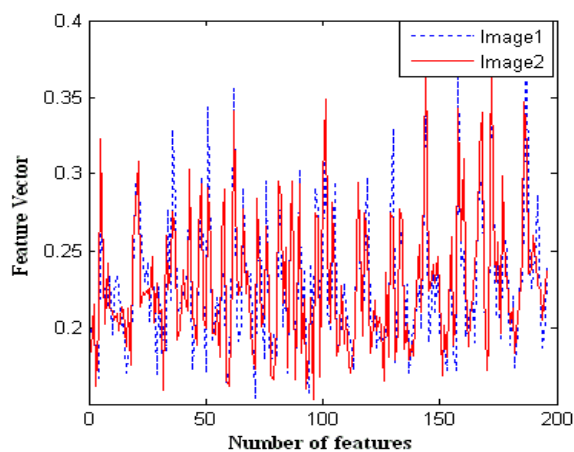


Fig. 6: Entropy Feature plot of two same users on PolyU database

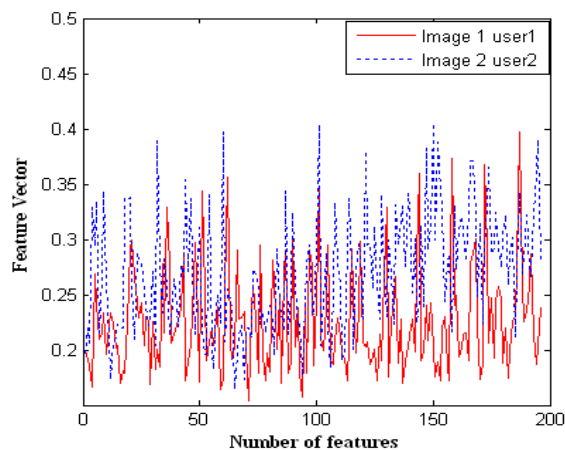


Fig. 7: Entropy Feature plot of the different user on PolyU database

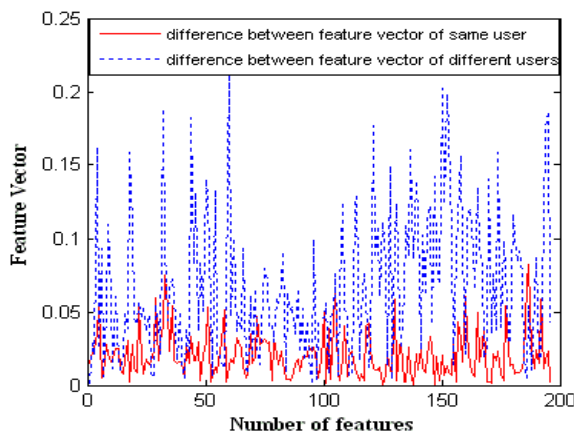


Fig. 8: The difference of Entropy feature vectors in Figs. 11 and 12 on PolyU database

TABLE III
ENERGY FEATURE ON IITD DATABASE

window size	ED	SVM using different Polynomial Kernel functions		
	% GAR at 10^{-2} FAR	1 degree	2 degree	3 degree
(4:1)*				
5x5	76	98.4	98.4	98.4
7x7	88	99.2	97.6	98.4
9x9	93.5	99.2	98.4	99.2
(3:2)*				
5x5	65.2	97.6	97.2	97.2
7x7	80.5	99.6	96.8	97.2
9x9	87.2	99.6	96.8	99.6

The results of authentication arising out of the three feature types due to all three different window sizes for the same number of training and testing samples (4:1) are depicted in Figs. 9 and 10 for PolyU and IITD database respectively. These plots reveal the fact that the Sigmoid and Entropy features yield the good authentication results over the Energy feature in both the classifiers. However it is not possible to compare both the classifiers because SVM only gives the classification accuracy but not the error unlike the Euclidean classifier and this error helps in drawing the ROC plot.

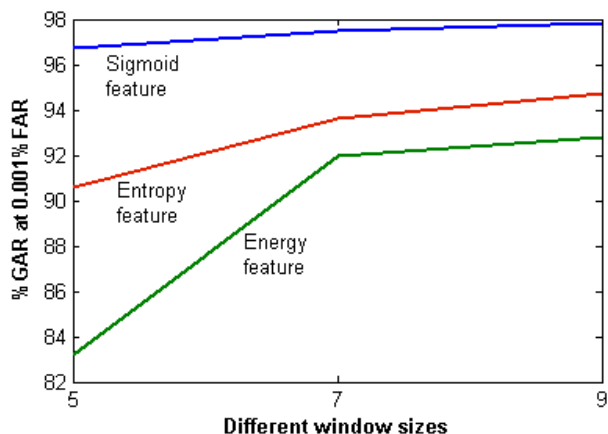


Fig. 9: Comparative plots of Sigmoid, Entropy and Energy features with window sizes (5x5, 7x7, 9x9) pixels with PolyU database (4:1) with Euclidean classifier.

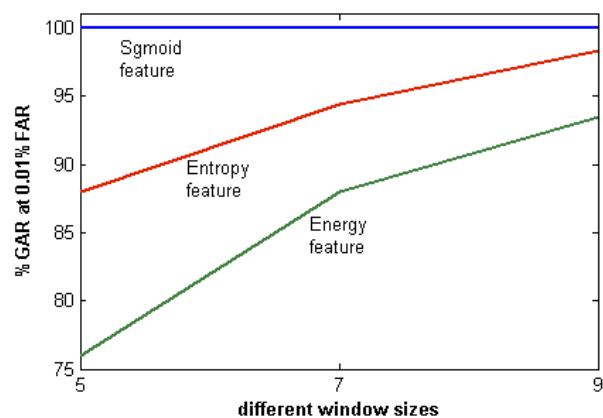


Fig. 10: Comparative plots of Sigmoid, Energy and Entropy features with window sizes (5x5, 7x7, 9x9) pixels with IITD data base (4:1) with Euclidean classifier.

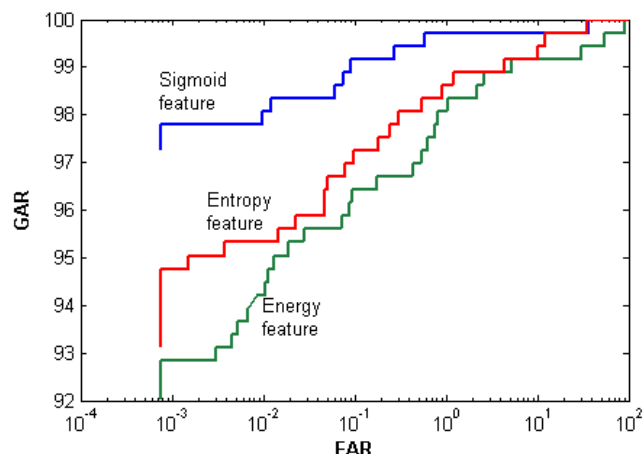


Fig. 11: Comparative ROC plots of Sigmoid, Entropy and Energy features with window sizes (9x9) pixels with PolyU data base (4:1)

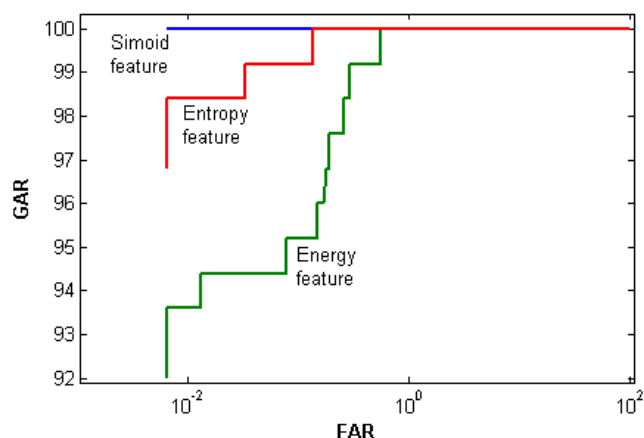


Fig. 11: Comparative ROC plots of Sigmoid, Entropy and Energy features with window sizes (9x9) pixels with IITD data base (4:1)

VI. CONCLUSIONS

A palmprint based biometric authentication system has been developed. Three feature types are experimented on the palmprints for suitability and usefulness for the palmprint based authentication. Of these the sigmoid and entropy features are found to be most suitable in terms of accuracy among all the feature types tested on the two databases. The energy features are lagging behind these two types of features.

The recognition rates of 100% are achieved with both sigmoid and entropy features on both the databases using SVM classifier. Irrespective of the type of features used, there is a marked difference in the results obtained using the Euclidean distance classifier and those with SVM classifier. SVM classifier with a linear kernel function and two polynomial kernels of degrees 2 and 3 perform with an accuracy of 100% recognition score on PolyU using sigmoid and entropy features.

The main problem for achieving very good authentication rates lies in the choice of the number of samples for both the training and the testing. We have made several experiments by varying these numbers. It is observed that as the training samples increase the matching scores increase but as the number of testing samples increase the matching scores decrease correspondingly. The *cross validation* is also done and the results are almost the same.

The future work will be concerned with developing new classifiers and new features along with the new membership functions.

REFERENCES

- [1] Xiang-Qian Wu, Kuan-Quan Wang, David Zhang, "Wavelet Based Palmprint Recognition", First international conference on Machine learning and cybernetics, Beijing, pp-1253-1257, 4-5 Nov 2002.
- [2] R. C. Gonzalez, R. E. Woods, Digital Image Processing, Addison Wesley publishers, 1993.
- [3] L. Hong and A. K. Jain, "Integrating Faces and Fingerprints for Personal Identification", IEEE Trans. on Pattern Analysis and Machine Intelligence, Vol. 20, No. 12, pp. 1295-1307, Dec 1998.
- [4] Anil K. Jain, Arun Ross and Salil Prabhakar, "An Introduction to Biometric Recognition", IEEE Trans. on Circuits and

System for Video Technology, Special Issue on Image and Video-Based Biometrics, Vol. 14, No. 1, January 2004.

- [5] N. Duta, A.K. Jain, and K.V. Mardia, "Matching of Palmprint," *Pattern Recognition Letters*, Vol.23, No. 4, pp. 477-485, 2001.
- [6] David Zhang, Wai-Kin Kong, Jane You, and Michael Wong, "Online Palmprint Identification", *IEEE Trans. Pattern Analysis & Machine Intelligence*, Vol. 25, No. 9, pp. 1041 – 1050, September 2003.
- [7] H. K. Polytechnic University, "Palmprint database", Biometric Research Center Website. 2005. <http://www4.comp.polyu.edu.hk/~biometrics/>.
- [8] H. Li, Y. Liang, and Q. Xu, "Support Vector Machines and its Applications in Chemistry", *Chemometrics and Intelligent Laboratory Systems*, vol. 95, pp. 188-198, Feb. 2009.
- [9] Chih-Chung Chang and Chih-Jen Lin, LIBSVM: a library for support vector machines, 2001. <http://www.csie.ntu.edu.tw/~cjlin/libsvm>
- [10] Li Fang, Maylor K.H. Leung, Tejas Shikhare, Victor Chan, Kean Fatt Choon, "Palmprint Classification", *IEEE Int. Conf. on Systems, Man and Cybernetics*, Vol. 4, 8-11 October 2006, pp.2965-2969.
- [11] E. Boonchien, W. Boonchieng, and R. Kanjanavani, "Edge-Detection and Segmentation Methods for Two-Dimensional Echocardiograms", *Proc. Int'l Conf. Computers in Cardiology*, pp. 541-544, September 2004.
- [12] Guang Dai and Changle Zhou, "Face Recognition Using Support Vector Machines with the Robust Feature", in *Proc. RO-MAN'03*, 2003, pp. 49-53.
- [13] Michael Goh Kah Ong, Connie Tee and Andrew Teoh Beng Jin, "Touch-less Palm-print Biometric System", in *Proc. VISIAPP'08*, 2008, pp. 423-430.
- [14] V.N. Vapnik, *Statistical Learning Theory*. New York: Wiley-Interscience, 1998.
- [15] B. Scholkopf, C.J.C. Burges, and A.J. Smola, *Advances in kernel Methods-Support Vector Learning*. Cambridge, MA: MIT Press, 1998.
- [16] M. Hanmandlu, H.M. Gupta, Neha Mittal, and S. Vasikarla, "An Authentication System Based on Palmprint", in *Proc. ITNG*, 2009, pp.399-404.